Structure, Volume *26*

Supplemental Information

Crystal Structure of Bicc1 SAM Polymer and Mapping of Interactions between the Ciliopathy-Associated Proteins Bicc1, ANKS3, and ANKS6

Benjamin Rothé, Catherine N. Leettola, Lucia Leal-Esteban, Duilio Cascio, Simon Fortier, Manuela Isenschmid, James U. Bowie, and Daniel B. Constam

Supplemental Data

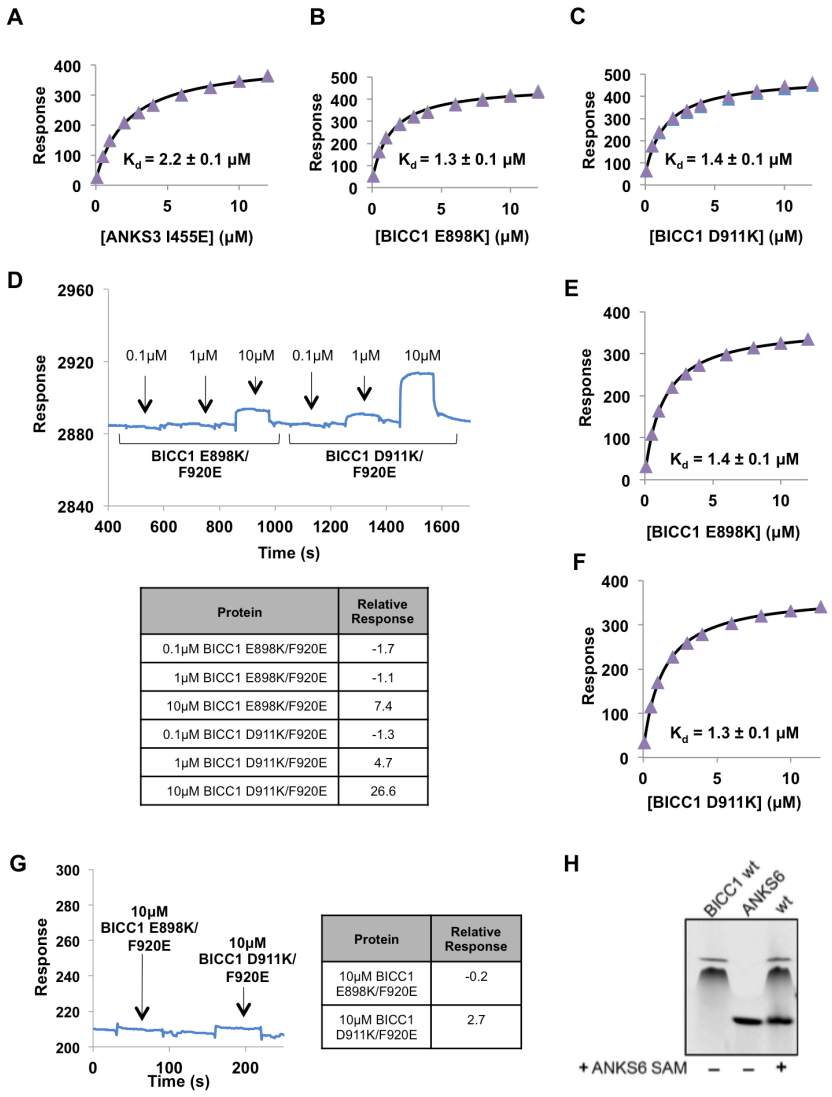

Protein	Relative Response
0.1μM BICC1 E898K/F920E	-1.7
1μM BICC1 E898K/F920E	-1.1
10μM BICC1 E898K/F920E	7.4
0.1μM BICC1 D911K/F920E	-1.3
1μM BICC1 D911K/F920E	4.7
10μM BICC1 D911K/F920E	26.6

Protein	Relative Response
10μM BICC1 E898K/F920E	-0.2
10μM BICC1 D911K/F920E	2.7

Figure S1, related to Figure 1: Affinity of Bicc1 SAM domain homotypic and heterotypic interactions. (A) SPR analysis of the binding affinity of soluble ML-mutant ANKS3 SAM I455E for immobilized EH-mutant Bicc1 SAM R924E. **(B, C)** SPR analysis of the binding affinities of soluble ML mutant Bicc1 E898K (B) or Bicc1 D911K (C) for immobilized EH-mutant ANKS3 F472E. **(D)** Raw Biacore data and relative response units of the Bicc1 SAM double mutants E898K/F920E and D911K/F920E flowed over an ANKS3 F472E SAM-conjugated Biacore chip. ANKS3 binding to BICC1 double mutants with mutations in both the ML and EH surfaces was close to background, demonstrating that ANKS3 and Bicc1 SAM domains associate via their ML and EH surfaces. **(E, F)** SPR analysis of the binding affinity of the native Bicc1 SAM interface was measured by equilibrium binding of the Bicc1 ML mutants E898K (E) or D911K (F) to immobilized Bicc1 EH mutant R924E. The Bicc1 SAM homotypic interaction has an average Kd = 1.35 ± 0.1 μM. **(G)** Raw Biacore data and relative response units of the Bicc1 double mutants E898K/F920E and D911K/F920E flowed over a Bicc1 R924E conjugated Biacore chip. Bicc1 double mutants defective in both the EH and ML surfaces exhibit minimal binding, demonstrating that the measured binding affinity is between a native ML and EH surface and not an alternate binding site. **(H)** negGFP native gel analysis of Bicc1 SAM and ANKS6 SAM alone (first two lanes) or together (third lane). For SPR, error bars of triplicate measurements that were fit to a 1:1 steady-state model are smaller than the data points.

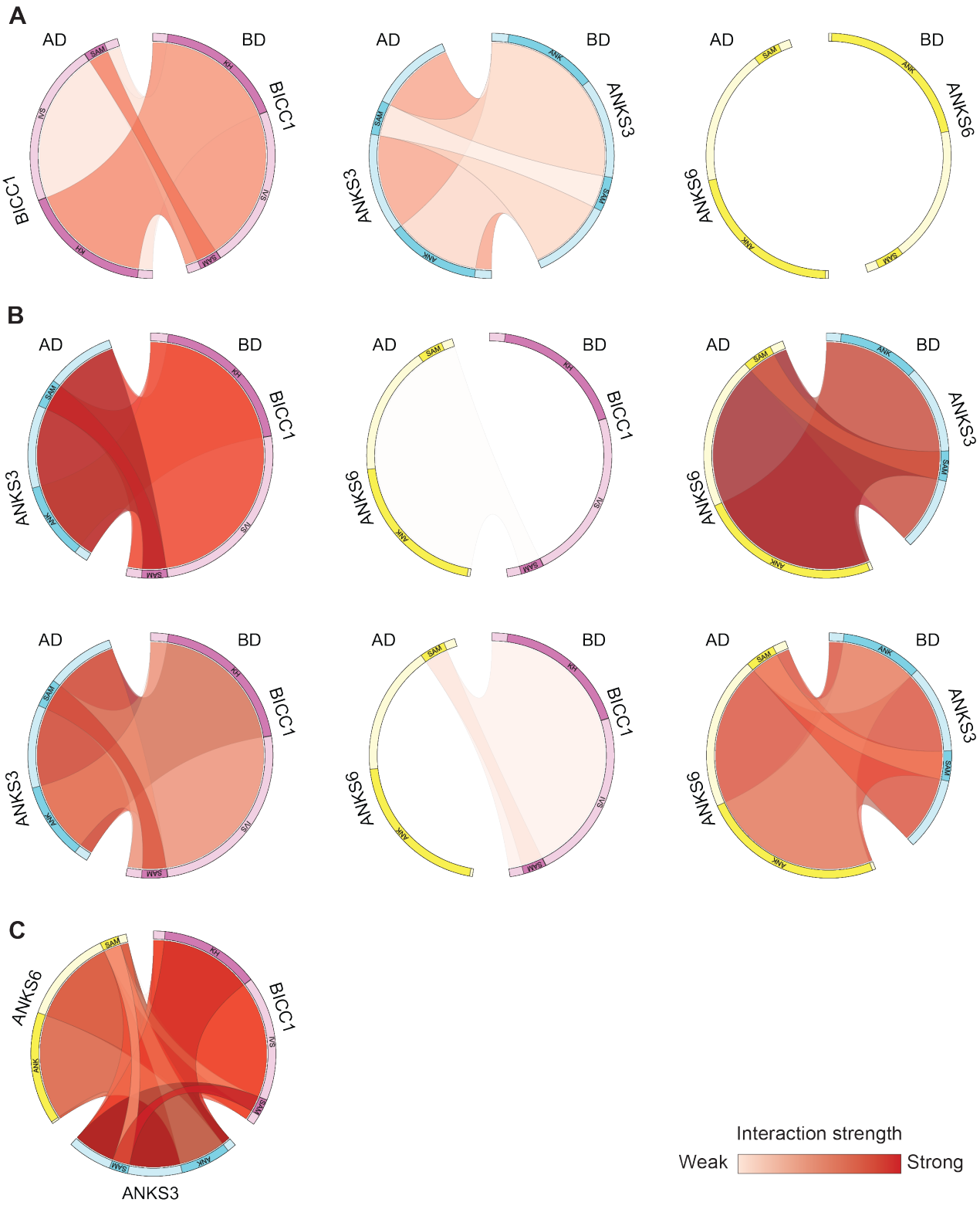

Figure S2, related to Figure 2: CIRCOS representation of the Y2H mapping. (A) CIRCOS representations of the relative strengths of self-interactions among specific regions within Bicc1, ANKS3 and ANKS6. **(B)** Details of interactions between the indicated pairs of proteins and their specific domains tested in both ways as bait (BD) and prey (AD). **(C)** Summary of the Bicc1-ANKS3-ANKS6 cross-interactions. The scale of interaction strengths (bottom right) was defined based on relative resistance to increasing concentrations of 3-AT, a competitive inhibitor of the reporter gene product.

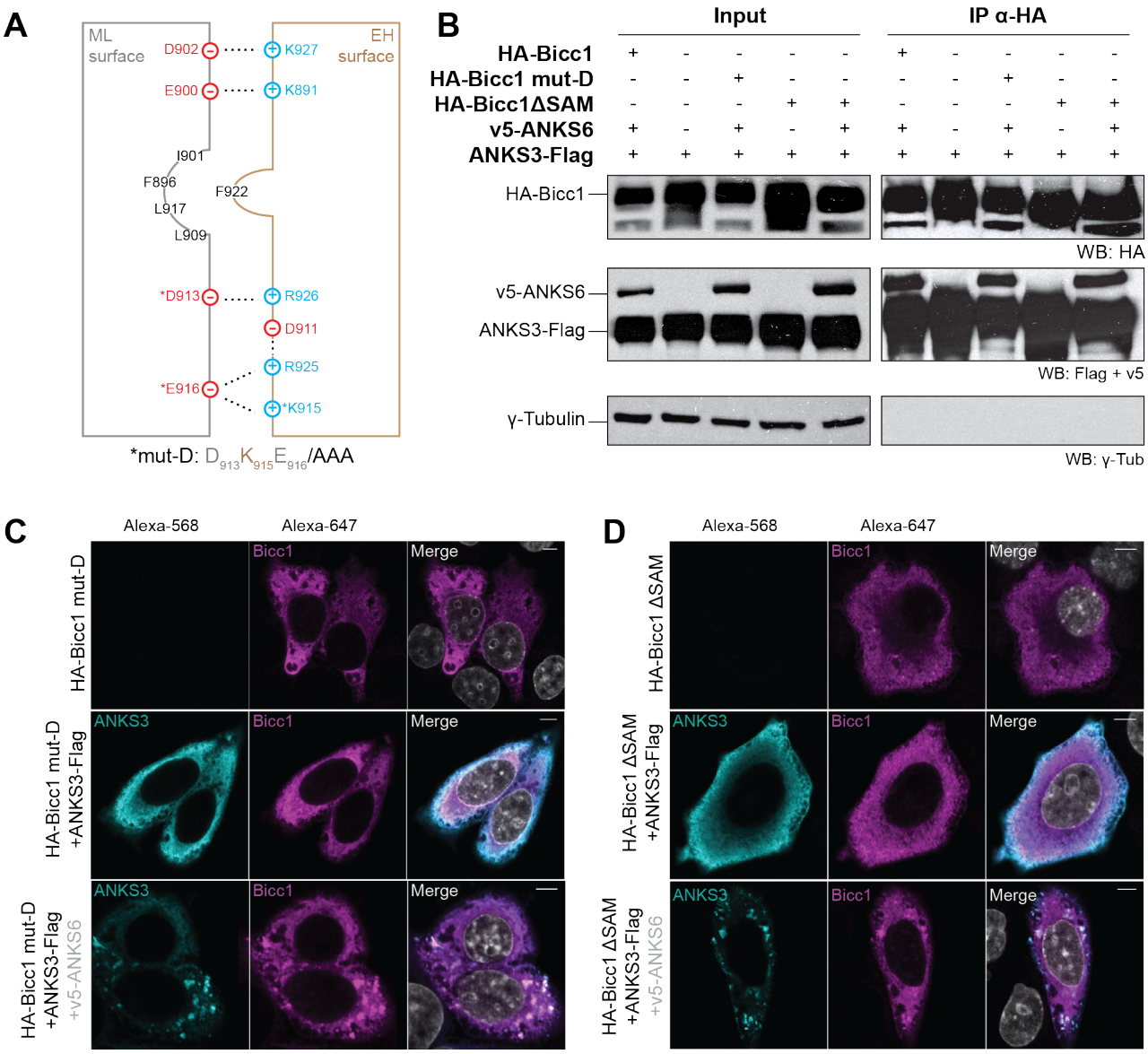

Figure S3, related to Figures 3 & 5: Bicc1 polymerization is not essential to bind ANKS3 and to form cytoplasmic foci with ANKS3 and ANKS6. (A) Graphical representation of the main amino acids involved in the Bicc1 SAM-SAM interface according the Bicc1-SAM crystal structure shown in Figure 1. **(B)** ANKS3-Flag, and v5-ANKS6 co-immunoprecipitation by HA-Bicc1 mut-D and ΔSAM in HEK293T cells. Five percent of total cell extracts were loaded as input. γ-tubulin was used as negative control. **(C, D)** Immunostaining of HA-Bicc1 mut-D and ΔSAM together with ANKS3-Flag with or without v5-ANKS6 in HeLa cells using anti-HA and anti-Flag antibodies. v5-ANKS6 was left unstained due to expected cross-reactivity of secondary antibodies. Bars, 5 μm.

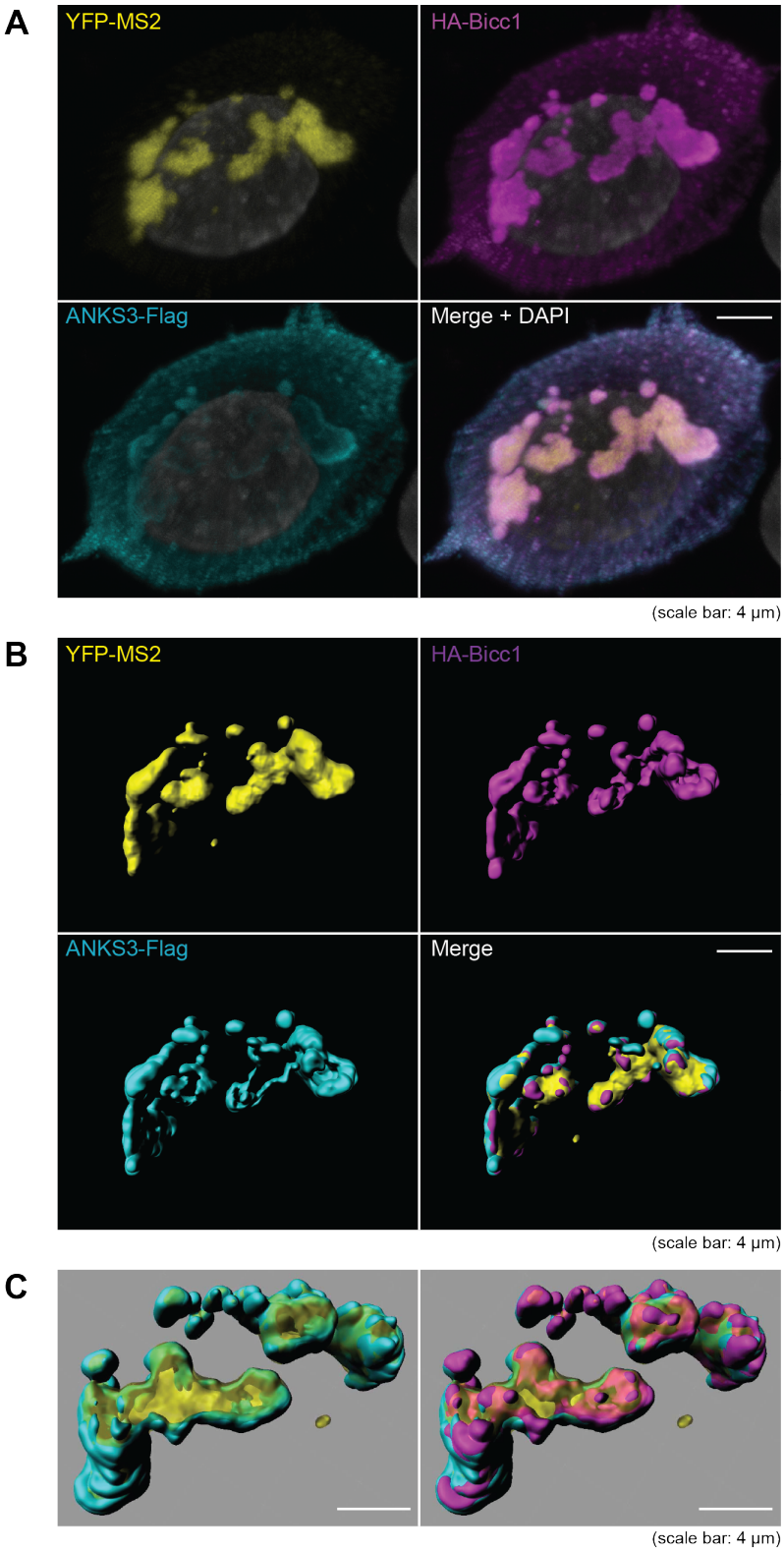

Figure S4, related to Figure 6D: 3D rendering of Bicc1-ANKS3-mRNA scaffolds. (A) Z-projection of the Luc-AC6-MS2×27 reporter mRNA and immunostained HA-Bicc1 and ANKS3-Flag in HeLa cells. The distribution of MS2-tagged mRNA was detected by monitoring the retention of nuclear MS2-YFP fusion protein in the cytoplasm. Bar, 4 μm. **(B)** 3D rendering of Bicc1-ANKS3-mRNA foci in panel A using Imaris software. Bar, 4 μm. **(C)** Enlarged and superimposed views of ANKS3-Flag and reporter RNA (left panel), or ANKS3-Flag, reporter RNA and HA-Bicc1 (right panel) after 3D rendering. Yellow color marking the reporter mRNA volume is transparent to not obscure the distribution of HA-Bicc1 (magenta) and ANKS3-Flag (blue) inside the foci. Bar, 4 μm.

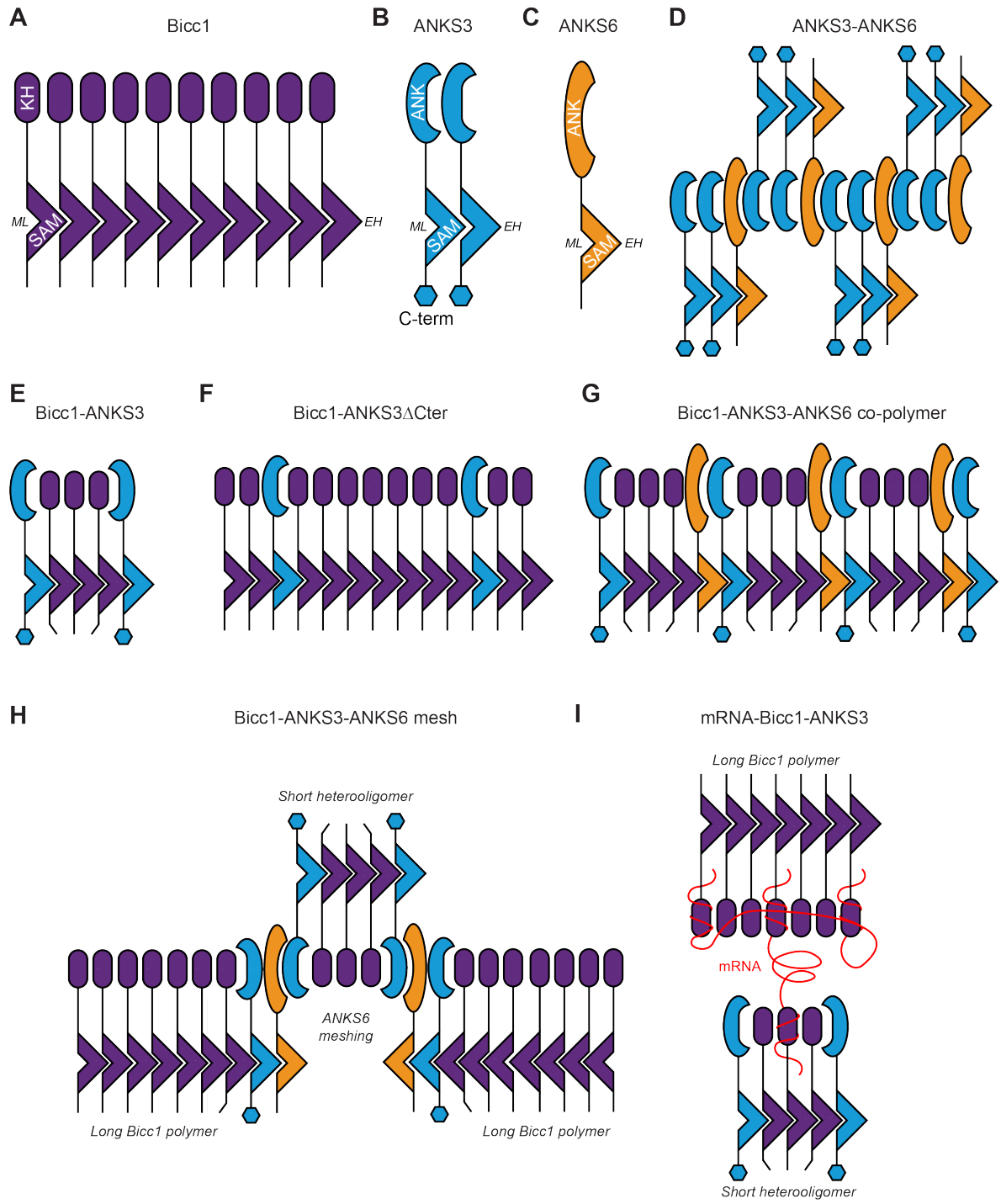

Figure S5, related to Figures 4, 5 & 6: Possible topologies of heterooligomeric scaffolds formed by Bicc1, ANKS3 and ANKS6. (A) Long Bicc1 homopolymer. **(B)** ANKS3 homooligomer, depicted here as a dimer because of its inability to form macroscopic cytoplasmic foci, although sucrose density fractionation suggests that SAM domains and ANK may interlink oligomer repeats. **(C)** ANKS6 monomer. **(D)** ANKS3-ANKS6 complex interfaced through SAM-SAM and ANK-ANK interactions. **(E)** Short Bicc1-ANKS3 heterooligomers capped on either side by ANKS3. **(F)** Model of how the deletion of the long C-terminal domain of ANKS3 may allow Bicc1-ANKS3ΔCter co-polymers to elongate further. **(G-H)** Models how ANKS6 co-recruitment may connect small Bicc1-ANKS3 heterooligomers into large Bicc1-ANKS3-ANKS6 scaffolds by co-polymerization or meshing, respectively. Bicc1 still associates with ANKS3-ANKS6 complexes even when polymerization of its own SAM domain is blocked by specific mutations, (panel D), consistent with KH domain binding to ANKS3 (**Figs. 2B, S3B**). **(I)** Bicc1-ANKS3 heterooligomers and Bicc1 homopolymers can be scaffolded into large ribonucleoprotein complexes by a Bicc1-bound mRNA.